Applied Thermal Engineering 183 (2021) 116178

Contents lists available at ScienceDirect

Applied Thermal Engineering

journal homepage: www.elsevier.com/locate/apthermeng

Greenhouse dehumidification by zeolite-based desiccant coated heat exchanger

Mohammad Amani, Majid Bahrami *

Laboratory for Alternative Energy Conversion (LAEC), School of Mechatronic Systems Engineering, Simon Fraser University, BC V3T 0A3, Canada

ARTICLE INFO

Keywords:
Greenhouse
Dehumidification
COP
Moisture removal
Desiccant-coated heat exchanger
Adsorption systems
Renewable energy sources

ABSTRACT

Desiccant-coated heat exchanger (DC-HX) is a promising technology for greenhouse dehumidification since both latent and sensible loads can be addressed simultaneously. DC-HX can be operated using low-grade heat, with temperatures less than 90 °C, from renewable energy sources, which makes them attractive from environmental and operating cost perspectives. In this study, a new DC-HX coated with AQSOA™-FAM-Z02 is built and studied experimentally and theoretically under typical greenhouse conditions for the first time. For this purpose, a custom-built experimental setup is developed to examine the dehumidification performance of the proposed DC-HX. The effects of greenhouse airflow rate, temperature, and relative humidity (RH), as well as regeneration and cooling heat transfer fluid (HTF) temperatures, on the average moisture removal capacity (MRC) and thermal coefficient of performance (COP) are analyzed. Moreover, the contributions of the removed latent and sensible heats by the present DC-HX are discussed. It is found that the custom-built DC-HX can achieve cyclic MRC and COP in the range of 2.5–4.0 and 0.18–0.3, thereby providing satisfactory dehumidification performance for greenhouse applications. Moreover, optimal operating parameters to maximize COP and MRC are determined by performing a multi-objective optimization using genetic algorithm approach.

1. Introduction

The agriculture and food sector is a considerable part of the Canadian economy [1]. Since 1990, this sector has been responsible for almost 5% of the total Canadian Gross Domestic Product [2]. Temperature and humidity in greenhouses are controlled using systems that mainly depend on fossil fuels and constitutes a significant operating cost for greenhouse growers in Canada. In 2005, about 260 million dollars of fuel was consumed by the Canadian greenhouse industry, i.e., 12% of their total revenue [3]. Thus, there is an immense desire for developing efficient heating, dehumidification, and cooling systems in greenhouses that can run on non-payable (or low-cost) renewable energy sources, including low-grade heat, geothermal, bioenergy, and solar thermal to reduce energy cost [4,5].

Humidity increment in greenhouses is inevitable due to plant transpiration. Excessive humidity causes plant diseases and deterioration of the crops [6]. Therefore, dehumidification plays a vital role in climate control of greenhouses. Amani et al. [7] presented a state-of-the-art review of the various dehumidification technologies available in the agricultural industry. They reported that ventilation is the simplest dehumidification method in greenhouses [7]. This method leads to significant heat loss during the cold season and thus increases heating costs. Maslak and Nimmermark [8] and Campen and Bot [9] reported that 20–30% of the thermal energy for climate control of greenhouses is due to ventilation, which indicates the need for developing energy-efficient dehumidification systems.

Solid-desiccant dehumidification systems can operate with low-grade thermal energy and can significantly reduce the electricity consumption [10,11]. Recently, desiccant-coated heat exchangers (DC-HXs) have been proposed as a new dehumidification system, and several researchers have evaluated their performances. Vivekh et al. [12] summarized the developments in DC-HXs and showed that the composite LiCl/silica gel desiccants performed better than pure silica gel. Saeed and Al-Alili [13] presented a review on the experimental studies and different modeling approaches of DC-HXs and reported that SAPO34 generally outperforms the silica gel. Oh et al. [14] and Li et al. [15] concluded that the air humidity content has a considerable impact on the overall mass transfer coefficient of the DC-HX. Zhao et al. [16] concluded that performance of a DC-HX equipped with a heat recovery device improved significantly compared to conventional cycle. Besides, Ge et al. [17], Valarezo et al. [18], and Hu et al. [19] considered

* Corresponding author.
E-mail address: mbahrami@sfu.ca (M. Bahrami).

https://doi.org/10.1016/j.applthermaleng.2020.116178
Received 2 July 2020; Received in revised form 27 August 2020; Accepted 25 September 2020
Available online 9 October 2020

Nomenclature

A	cross-sectional area (m^2)
C	perimeter of flow passage (m)
COP	thermal coefficient of performance
c_p	specific heat (J/kg K)
$DC\text{-}HX$	desiccant-coated heat exchanger
D_t	transient moisture removal (g/kg)
f	mass per unit length (kg/m)
h	convection heat transfer coefficient (W/m^2 K)
h_v	heat of vaporization (kJ/kg)
K_y	convection mass transfer coefficient (kg/m^2 s)
$\dot{m}$	mass flow rate (kg/s)
MRC	moisture removal capacity (g/kg)
P	pressure (Pa)
$\dot{Q}$	heat transfer rate (W)
q_{st}	isosteric heat of adsorption (kJ/kg)
RH	relative humidity (%)
T	temperature (°C)
t	time
u	velocity (m/s)
W	desiccant water uptake (kg adsorbate/kg adsorbate)
$\dot{W}$	power (W)
Y	humidity ratio (kg/kg)

Greek letters

ρ	density (kg/m^3)

Subscripts

a	air
atm	atmosphere
c	cold
d	desiccant
h	hot
lat	latent
m	heat exchanger matrix
reg	regeneration
sen	sensible
v	water vapor
vs	saturated water vapor
w	heat transfer fluid (water)

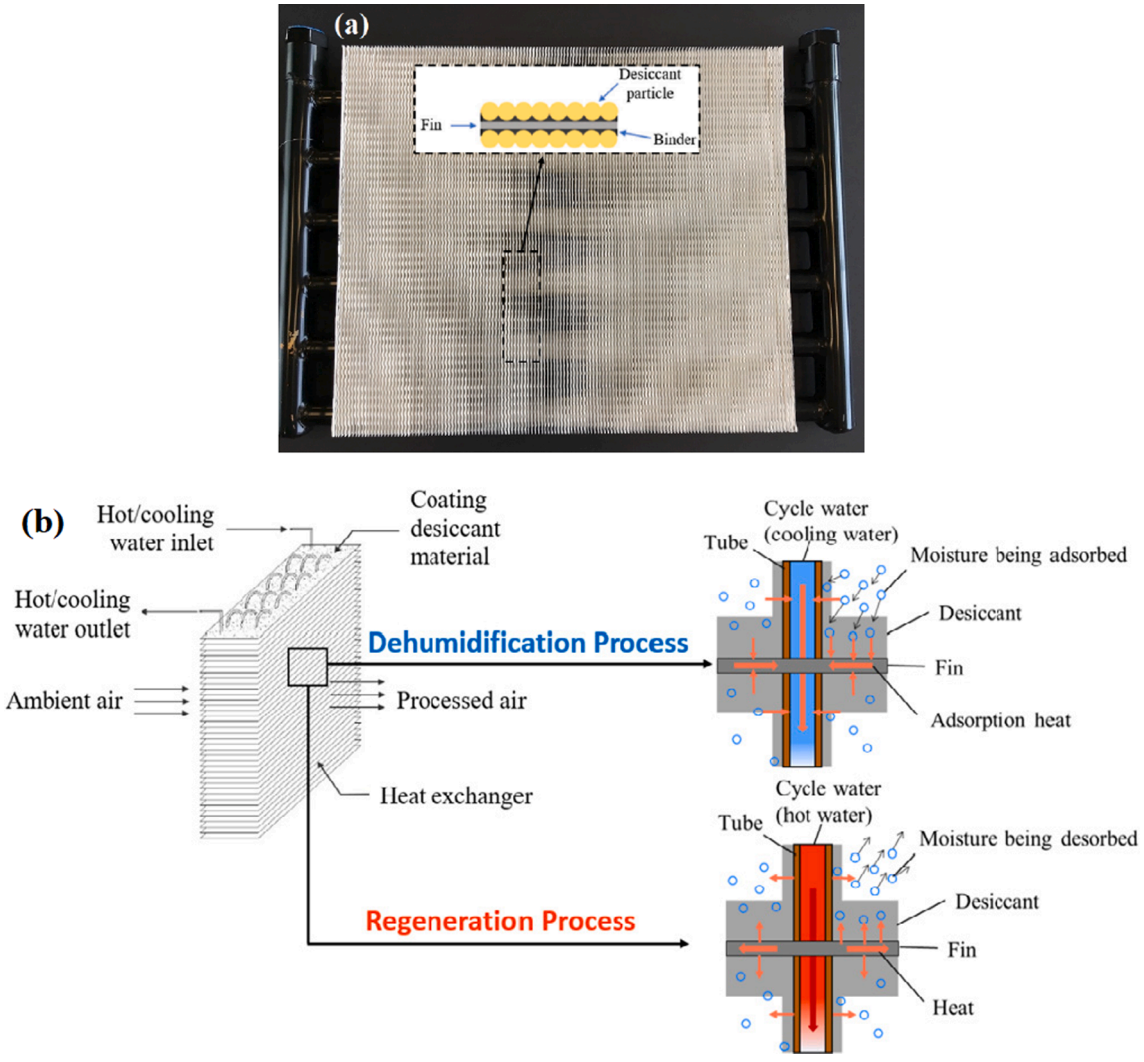

Fig. 1. (a) Picture of our DC-HX; (b) schematic of DC-HX and its working principle [22].

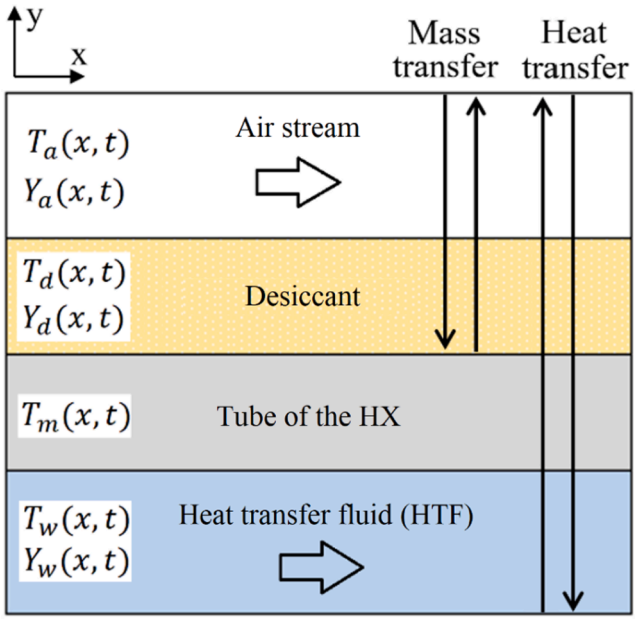

Fig. 2. Control volume considered in the present model.

composite DC-HXs including silica gel/potassium formate, silica gel/sodium acetate, and silica gel/lithium chloride composite desiccant-based heat exchangers and found that the dehumidification capacity improved significantly compared to pure silica gel-based DC-HX. In addition, Ge et al. [20,21] developed mathematical model to predict the performance of DC-HX and evaluated the effects of main operation parameters and climatic conditions.

To the best of authors' knowledge, the open literature on DC-HX systems is mainly focused on the performance of silica gel-based DC-HXs. Thus, the objective of this work is to evaluate the feasibility of a new AQSOA™-FAM-Z02 DC-HX for greenhouse dehumidification. A theoretical modeling, experimental analysis, and a parametric study are performed to investigate the effects of operating variables such as air flow rate, temperature, and RH, as well as regeneration and cooling heat transfer fluid (HTF) temperatures, on the average moisture removal capacity (MRC) and thermal coefficient of performance (COP) of the proposed DC-HX. Moreover, contributions of latent heat and sensible heat removed by DC-HX are presented. Finally, optimal operating conditions to maximize COP and MRC are established by performing a multi-objective optimization using a genetic algorithm.

2. Operating principle of DC-HX

In a DC-HX, the desiccant is coated on the fins of a fin-tube heat exchanger, see Fig. 1(a). The process air passes over the fin side of the heat exchanger. In DC-HX, cold HTF is circulated through the heat exchanger during the adsorption process to remove the generated adsorption heat and improve the desiccant's adsorption performance. Once the desiccant is saturated, the adsorbed water vapor should be removed from the desiccant during the desorption process. For this purpose, hot HTF is pumped into the heat exchanger to carry out the regeneration process. Fig. 1(b) schematically shows the working principle of a DC-HX.

2.1. Theoretical modeling

A theoretical model is developed to predict the dynamic performance of a DC-HX. As shown in Fig. 2, the control volume considered in our modeling consists of the air stream, coated desiccant, the heat exchanger fin, and HTF. This is a complex transient, conjugate heat and mass transfer process and to develop a theoretical solution, the following

Table 1
Governing equations based on mass and energy conservations.

	Governing equations
Mass balance in the air stream	$\rho_a A_a\left(\frac{\partial Y_a}{\partial t}+u_a\frac{\partial Y_a}{\partial x}\right)+f_d\frac{\partial W}{\partial t}=0$
Mass balance in the desiccant	$f_d\frac{\partial W}{\partial t}=K_y C(Y_a-Y_d)$
Energy balance in the air stream	$\rho_a A_a c_{pa}\left(\frac{\partial T_a}{\partial t}+u_a\frac{\partial T_a}{\partial x}\right)=hC(T_d-T_a)+K_y C c_{pv}(Y_d-Y_a)(T_d-T_a)$
Energy balance in the HTF stream	$\rho_w A_w c_{pw}\left(\frac{\partial T_w}{\partial t}+u_w\frac{\partial T_w}{\partial x}\right)=h_w C_w(T_d-T_w)$
Energy balance in the whole unit	$\rho_a A_a c_{pa}\left(\frac{\partial T_a}{\partial t}+u_a\frac{\partial T_a}{\partial x}\right)+\rho_w A_w c_{pw}\left(\frac{\partial T_w}{\partial t}+u_w\frac{\partial T_w}{\partial x}\right)+\left[f_d(c_{pd}+Wc_{pw})+f_m c_{pm}\right]\frac{\partial T_d}{\partial t}=K_y C(Y_a-Y_d)q_{st}$
Relationship between humidity ratio and RH	$Y_d=\frac{0.622P_v}{(P_{atm}-P_v)}=\frac{0.622RH_d}{P_{atm}/P_{vs}-RH_d}P_{vs}=\exp(23.196-\frac{3816.44}{T_d+227})$
Initial conditions	$T_{a,t=0}=T_{a,in}$, $Y_{a,t=0}=Y_{a,in}$, $T_{d,t=0}=T_{a,in}$, $Y_{d,t=0}=Y_{a,in}$, $T_{w,t=0}=\begin{cases}T_{c,in} & \text{for adsorption process}\\ T_{h,in} & \text{for desorption process}\end{cases}$
Boundary conditions	$T_{a,x=0}=T_{a,in}$, $Y_{a,x=0}=Y_{a,in}$, $T_{w,y=0}=\begin{cases}T_{c,in} & \text{for adsorption process}\\ T_{h,in} & \text{for desorption process}\end{cases}$

Table 2
Spline fitting coefficients proposed by Goldsworthy [23].

Desiccant	W_m	Reference isotherm	Heat of adsorption
AQSOA™-FAM-Z02	0.330	$W_l=0.01, W_u=0.16$	$W_l=0.01, W_u=0.95$
		$a_0=-10.7991$, $a_1=129.2088$, $a_2=-761.0932$, $a_3=1632.8661$	$b_0=3.1138$, $b_1=-31.9928$, $b_2=224.9962$, $b_3=-808.2050$, $b_4=1633.2722$, $b_5=-1874.8762$, $b_6=1138.7631$, $b_7=-283.9005$
		$W_l=0.16, W_u=0.9$	
		$a_0=-3.0315$, $a_1=11.0993$, $a_2=-26.3034$, $a_3=21.3185$	

simplifying assumptions are made:

- Thermophysical properties of the desiccant, HTF and the heat exchangers (tubes and fins) remain constant.
- Uniform inlet air conditions.
- Airflow is considered fully-developed over the heat exchanger. Thus, heat and mass transfer coefficients are considered constant over time.
- Adsorption heat is released at the interface between the air stream and the desiccant film.

The heat and mass transfer in DC-HXs are modeled by applying energy and moisture balance in the air stream and in the desiccant layer. The governing equations based on mass and energy conservations for each control volume, as well as the initial and boundary conditions, are listed in Table 1.

Goldsworthy [23] proposed the following spline functions for isotherms and isosteric heats of adsorption for AQSOA™-FAM-Z02 over the adsorption capacity between the lower (W_l) and upper (W_u) bounds.

$$ln\left(\frac{P(W)}{P_{sv}}\right)=\sum_{i=0}^{n}a_i\left[W-W_l\right]^i \quad \text{for } W_l\le W\le W_u \tag{1}$$

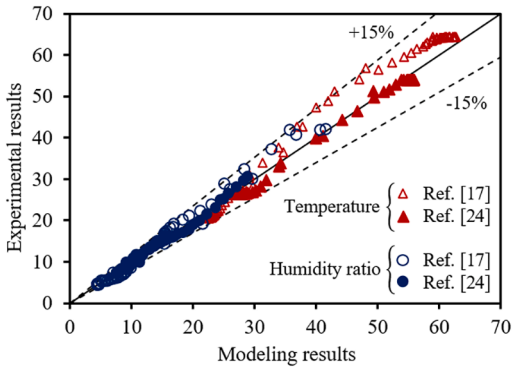

Fig. 3. Comparison between the present model and experimental data for silica gel-based DC-HX published by [17,24].

$$\frac{q_{st}}{H_v} = \sum_{i=0}^{n} b_i \left[W - W_l \right]^i \quad \text{for } W_l \le W \le W_u \tag{2}$$

where $W = W/W_m$ is the normalized adsorption capacity and H_v represents the heat of vaporization. The values of the coefficients are given in Table 2. These correlations are used in the present model.

2.2. Numerical solution and verification

An in-house finite volume code was prepared to solve the coupled moisture and energy equations, listed in Table 1, using a fourth-order Runge-Kutta iteration method in MATLAB software. As a first step to validate the developed model, our results are compared against the experimental results obtained by Ge et al. [17,24] for a silica gel-based DC-HX over a range of operating conditions (air temperature of 10–30°C, air humidity ratio of 8–15 g/kg, and hot HTF temperature of 60–90°C). Fig. 3 shows that the present model results are in good agreement with the experimental data of Ge et al. [17,24], the majority of data are within ±15% of the predicted results.

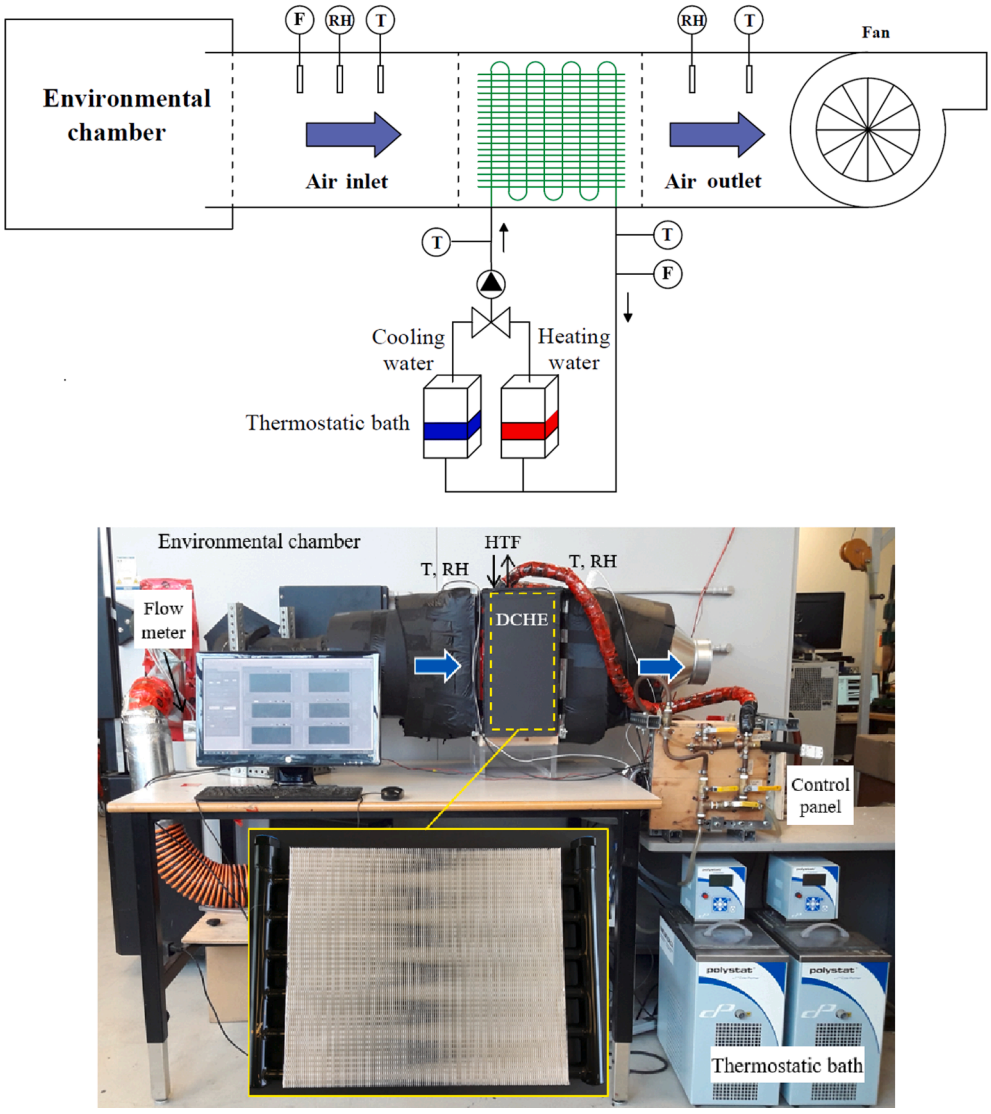

Fig. 4. (a) Schematic view and (b) photographic image of the experimental setup including the proposed DC-HX, environmental chamber, air duct, fan, two circulating baths, location of sensors and a data acquisition system.

Table 3
Specifications of the DC-HX.

Parameter	Value
Heat exchanger dimensions	305 × 355 × 38 (mm)
Fin thickness	0.1 (mm)
Fin pitch	2.3 (mm)
Desiccant weight	800 (g)
Tube diameter	8.25 (mm)
Fin material	Aluminium
Tube material	Copper
Desiccant thickness	0.3 (mm)

2.3. Performance metrics

To assess the dehumidification performance of the present DC-HX, the commonly-used MRC and COP parameters are used in this study.

MRC is defined as the time-averaged moisture removal during the adsorption process as follows [25]:

$$MRC = \frac{1}{t}\int_0^t D_t dt \tag{3}$$

where D_t is the transient moisture removal and is calculated as:

$$D_t = Y_{a,in} - Y_{a,out} \tag{4}$$

where $Y_{a,in}$ and $Y_{a,out}$ (g/kg) denote the air stream inlet and outlet humidity ratio during the adsorption process, respectively.

The second parameter pertains to efficiency-related index, which is thermal COP. It reflects the average air side latent heat removal during effective dehumidification process ($\dot{Q}_{lat}$) over the average heat exchanged of HTF in effective regeneration process ($\dot{Q}_{reg}$). The total input thermal energy is the thermal energy of hot HTF to heat up the desiccant material to release the moisture. The electrical power input of the fans and pumps is neglected for heat energy is the primary source of energy. COP can be computed using following equation [14]:

$$COP = \frac{\dot{Q}_{lat}}{\dot{Q}_{reg}} = \frac{\dot{m}_a\left(Y_{a,in} - Y_{a,out}\right)h_v}{\dot{m}_w c_{pw}\left(T_{w,in} - T_{w,out}\right)} \tag{5}$$

where $\dot{m}_a$ and $\dot{m}_w$ are the mass flow rate of the adsorption/regeneration air and hot HTF respectively, h_v is the vaporization heat of HTF, $T_{w,out}$ and $T_{w,in}$ are the respective temperature of hot HTF at inlet and outlet of the heat exchanger, and c_{pw} is the specific heat of the hot HTF at constant pressure.

It should be noted that DC-HX uses desiccant material and inner cooling source to remove the latent heat load and sensible heat load respectively, which are calculated by the following equations.

$$\dot{Q}_{lat} = \dot{m}_a\left(Y_{a,in} - Y_{a,out}\right)h_v \tag{6}$$

$$\dot{Q}_{sen} = \dot{m}_a c_{p,a}\left(T_{a,out} - T_{a,in}\right) \tag{7}$$

where $c_{p,a}$ is the specific heat of the air.

The average heat transfer on the HTF side in regeneration process is calculated by the following expression.

$$\dot{Q}_{reg} = \dot{m}_w c_{pw}\left(T_{w,in} - T_{w,out}\right) \tag{8}$$

3. Experimental study

3.1. Desiccant material

AQSOA™-FAM-Z02 is one of the promising adsorbents introduced for air-conditioning applications by Mitsubishi Chemical Ltd. [26]. It is durable, non-toxic, and environmentally-friendly, which makes it a suitable option for greenhouse dehumidification. The isotherms of FAM-Z02 measured by thermo-gravimetric vapor adsorption analyzer can be found in Refs. [23,27,28]. It was reported that its isotherm has a S-shaped curve and is a strong function of regeneration temperature.

Table 4
Operating variables for DC-HX performance testing; baseline values.

Parameters	Baseline condition	Varied range
Airflow rate	40 CFM	20–80 CFM
Air temperature	20°C	10–30°C
Air relative humidity	60%	40–90%
Cooling HTF temperature	10°C	5–30°C
Hot HTF temperature	70°C	50–90°C

3.2. Experimental system description

In this study, a custom-made experimental apparatus was built to measure the dehumidification characteristics of AQSOA™-FAM-Z02 DC-HX. Fig. 4 shows the schematic and an image of the testbed, the specifications of the DC-HX are list in Table 3.

An environmental chamber (Thermotron© Model XSE-3000-10-10) was used to mimic the greenhouse air condition. The air stream was supplied by a fan connected to the environmental chamber. A voltage regulator was employed to adjust the airflow rate. The air temperature, RH, and flow rate, as well as HTF temperature and flow rate at the inlet and outlet of the heat exchanger were measured. The collected data were recorded and further processed using LABVIEW software [29] with a sampling interval of 3 s. The humidity and temperature sensors of Vaisala-HMP110 and PT100 were used with an accuracy of ±0.1°C and ±1.5%RH, respectively, to measure the air RH and temperature of air and HTF. An orifice plate (4″ Oripac© model 4150) was employed with an accuracy of ±0.25% of the measured value to measure the airflow rate through pressure differential. Two Cole-Parmer® Polystat®

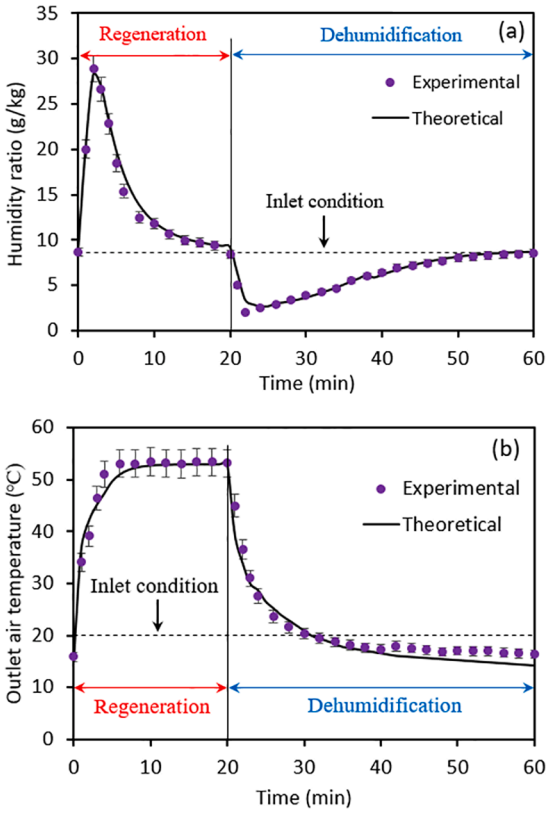

Fig. 5. Comparison between the present model and collected experimental data; (a) air stream outlet humidity ratio and (b) air stream outlet temperature over time.

cooling/heating circulating baths were used to achieve a constant regeneration and cooling HTF temperatures.

3.3. Uncertainty analysis

The method proposed by Kline and McClintock [30] is used to compute the uncertainty of the present experimental data as follows.

$$\Delta y = \left[\left(\frac{\partial f}{\partial x_1}\Delta x_1\right)^2 + \left(\frac{\partial f}{\partial x_2}\Delta x_2\right)^2 \cdots + \left(\frac{\partial f}{\partial x_n}\Delta x_n\right)^2\right]^{\frac{1}{2}} \quad (9)$$

$$\frac{\Delta y}{y} = \left[\left(\frac{\partial f}{\partial x_1}\frac{\Delta x_1}{y}\right)^2 + \left(\frac{\partial f}{\partial x_2}\frac{\Delta x_2}{y}\right)^2 \cdots + \left(\frac{\partial f}{\partial x_n}\frac{\Delta x_n}{y}\right)^2\right]^{\frac{1}{2}} \quad (10)$$

where, x_1, x_2 etc. are the independent variables of f function, Δx_1, Δx_2 etc. denote the absolute error of variables and $\Delta y/y$ represents the relative error. The analysis reveals that the uncertainties of measured MRC and COP in this study are 8.4% and 10.3%, respectively.

4. Results and discussion

The dynamic performance of DC-HX in terms of air stream outlet humidity ratio and temperature is evaluated. We also investigated the effects of operating parameters on the MRC, COP, latent heat, and sensible heat of the present DC-HX. For this purpose, using the developed model described in Section 2.1 and experimental analysis, only one variable is varied, while the others are maintained constant at the baseline values. The baseline values for the parameters are selected rather arbitrarily and are listed in Table 4. Furthermore, a multi-objective optimization is performed using a genetic algorithm to determine maximize values for COP and MRC.

4.1. Dynamic performance evaluation

As shown in Fig. 5, the dynamic performance of the present DC-HX under the baseline condition is analyzed in terms of air stream outlet humidity ratio and temperature. The following can be concluded:

- Experimental data and theoretical results agree well, with an average relative difference of ±15%.
- As expected, the air stream outlet humidity ratio drops remarkably at the beginning of the adsorption process due to hygroscopic characteristics of the desiccant material. Then, the humidity ratio reaches its minimum value of 2.0 g/kg in about 90 s and gradually increments to the inlet condition (8.8 g/kg) and approaches its saturation condition.
- During the regeneration process, the air stream outlet humidity ratio increases significantly and reaches its highest value of 28.8 g/kg; then it gradually decreases to its initial condition. The average air stream outlet humidity ratio was 5.8 g/kg during these tests, or in other words, MRC value was calculated as 3.0 g/kg.
- Regarding the air stream outlet temperature, it can be seen that the air temperature at the beginning of adsorption is high (53.5°C), because the DC-HX has just been switched from regeneration mode. Then, it rapidly decreases due to the cooling effect of cooling HTF and reaches to 16.5°C. The average supplied air temperature in the adsorption process is obtained 20.9°C.
- The adsorption/regeneration capacity of desiccant drops notably at the end of their corresponding processes, and interrupting/reversing the process at a particular stage would be beneficial in terms of efficiency. Thus, the duration of the adsorption/regeneration process must be selected such that the transient moisture removal (D_t) is significant. There exists a cycle time to achieve an optimal DC-HX performance. The following criteria is adopted to determine the effective cycle time: the variation of D_t and air stream outlet temperature at each time step should become no less than 3%, where the adsorption/regeneration cycle time will be 40 and 20 min, respectively. As can be seen, the effective time for regeneration is much shorter than the corresponding adsorption time. This is due to the fact that in regeneration process, the greater temperature difference between the HTF and inlet air means greater driven force. So it costs shorter time to turn the saturated desiccant into dry condition needed in regeneration stage compared with the time to turn dry desiccant into saturated condition in adsorption stage.

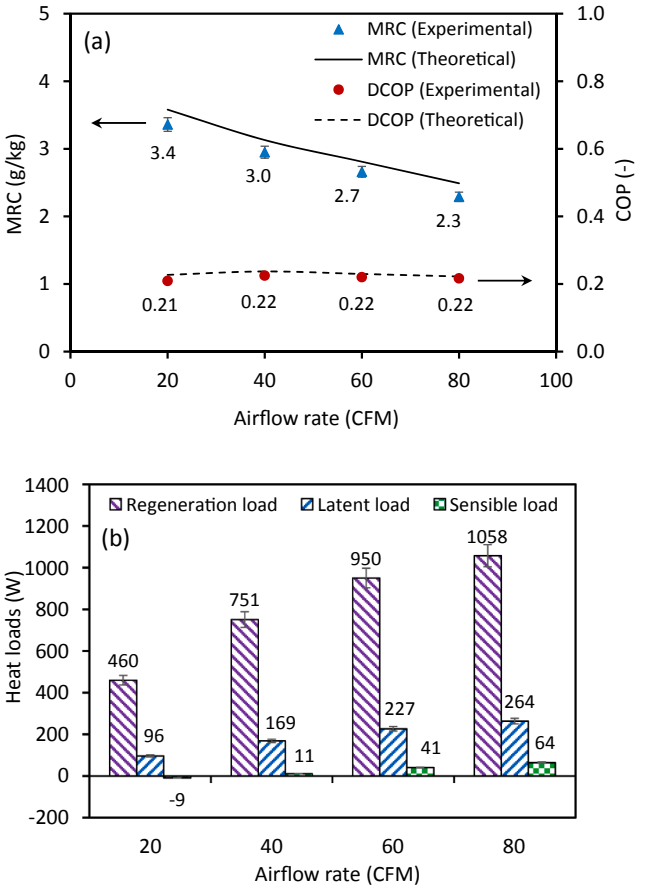

Fig. 6. Effect of airflow rate on the (a) MRC and COP obtained by theoretical and experimental analyses and (b) heat loads of DC-HX including required regeneration heat, latent heat removal from the greenhouse and sensible heat added to the greenhouse.

4.2. Effect of airflow rate

The effect of the airflow rate on the MRC, COP, latent heat, sensible heat, and regeneration heat of the present DC-HX is shown in Fig. 6. The following can be observed:

- MRC decreases from 3.4 to 2.3 g/kg with an increment of airflow rate from 20 to 80 CFM. This is because more air is introduced for dehumidification and the residence time of the air in contact with the desiccant gets shortened at higher airflow rates. Accordingly, the mass transfer process may not be efficient.
- COP varies marginally over the considered airflow rate. The increase of latent heat removal from the greenhouse and the required regeneration heat at higher airflow rates leads to the almost constant COP.
- Latent, sensible, and regeneration loads rise by elevating supplied airflow rate. This is because that higher inlet air velocity enhances the convection heat transfer between the fin and the air.

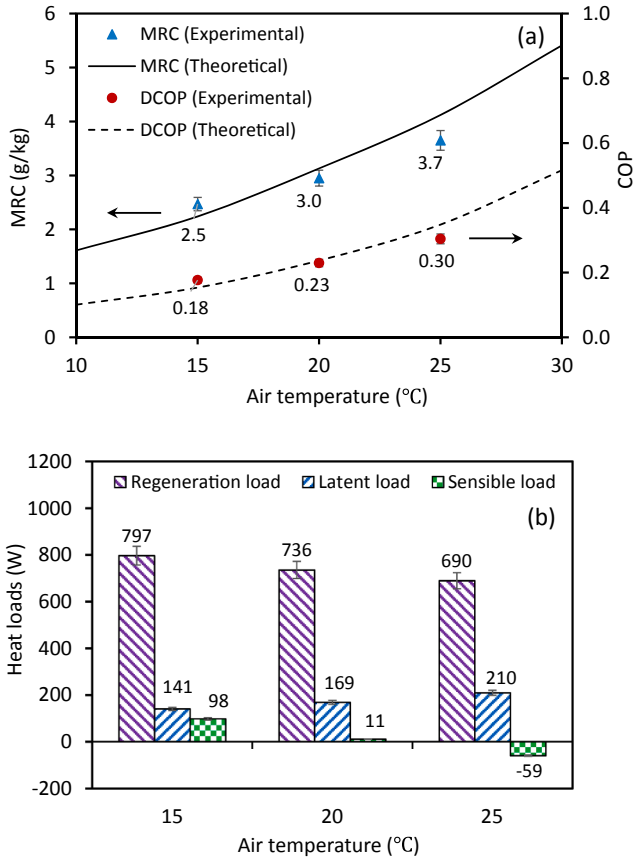

Fig. 7. Effect of air temperature on the (a) MRC and COP obtained by theoretical and experimental analyses and (b) heat loads of DC-HX including required regeneration heat, latent heat removal from the greenhouse and sensible heat added to the greenhouse.

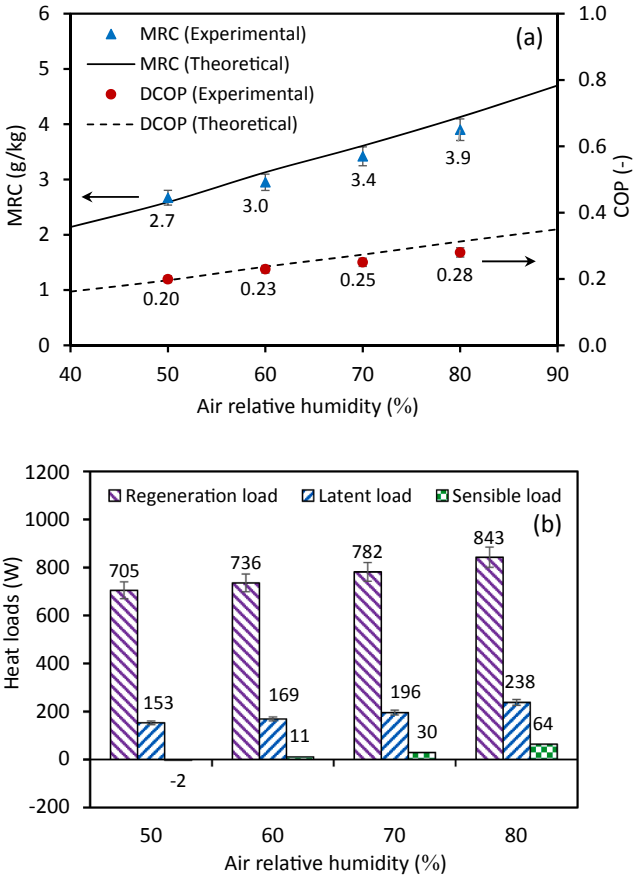

Fig. 8. Effect of air RH on the (a) MRC and COP obtained by theoretical and experimental analyses and (b) heat loads of DC-HX including required regeneration heat, latent heat removal from the greenhouse and sensible heat added to the greenhouse.

- Bigger flow rate is recommended to increase the temperature of supply air, indoor air circulation rate and COP.
- Sensible load for the airflow rate of 20 CFM is negative, indicating that the greenhouse air is cooled, while at higher airflow rates, the sensible heat is positive, i.e. heating the greenhouse.

4.3. *Effect of air temperature*

The majority of greenhouse crops generally prefer a healthy temperature range of 15–25°C for the best growth, depending on the species. Thus, the effect of air temperature on the MRC, COP, latent heat, sensible heat, and regeneration heat of the present DC-HX is illustrated in Fig. 7. The following can be concluded:

- Both MRC and COP increase with increasing air temperature, while RH remains constant. The reason is that the air holds more water vapor at elevated temperatures, thereby improving the moisture transfer. For example, when greenhouse air temperature increases from 15 to 25°C, MRC and COP increase from 2.5 to 3.7 g/kg and 0.18 to 0.30, respectively.
- Latent heat removal from the greenhouse improves in case of higher air temperature due to the increase of moisture transfer.
- Required load for the regeneration of desiccant decreases with an increase of the air temperature.
- Sensible heat added to the greenhouse decreases at higher air temperatures and sensible cooling is observed at the air temperature of 25°C.

4.4. *Effect of air relative humidity*

The effects of varying air RH from 50 to 80% on the MRC, COP, latent heat, sensible heat, and regeneration heat of the present DC-HX are shown in Fig. 8. The following can be concluded:

- MRC and COP increase with increasing air RH.
- When air RH increases from 50 to 80%, MRC increases from 2.7 to 3.9 g/kg, i.e., a 44% improvement. RH increase results in higher moisture content in air and improves the driving force for moisture transfer, thereby enhancing the dehumidification performance.
- COP enhances from 0.20 to 0.28, because of the increase in latent heat removal capacity, which shows greater efficiency of the DC-HX under high humidity conditions.
- Latent, sensible, and regeneration loads rise by elevating air RH.

4.5. *Effect of cooling HTF temperature*

The effect of cooling HTF temperature on the dehumidification performance of DC-HX in terms of MRC, COP, latent heat, sensible heat, and regeneration heat of the present DC-HX is depicted in Fig. 9. The following can be concluded:

- The adsorption heat is produced by the DC-HX during dehumidification process. This adsorption heat is continuously removed by circulating cooling HTF.
- MRC and COP increase slightly with the decrease in cooling HTF temperature. As it declines from 25 to 10°C, the MRC increases from

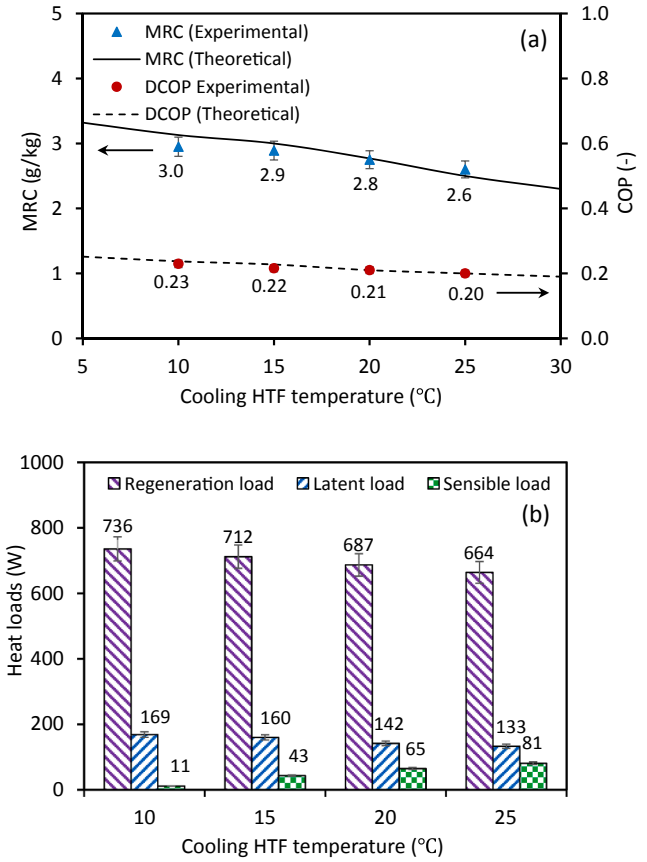

Fig. 9. Effect of cooling HTF temperature on the (a) MRC and COP obtained by theoretical and experimental analyses and (b) heat loads of DC-HX including required regeneration heat, latent heat removal from the greenhouse and sensible heat added to the greenhouse.

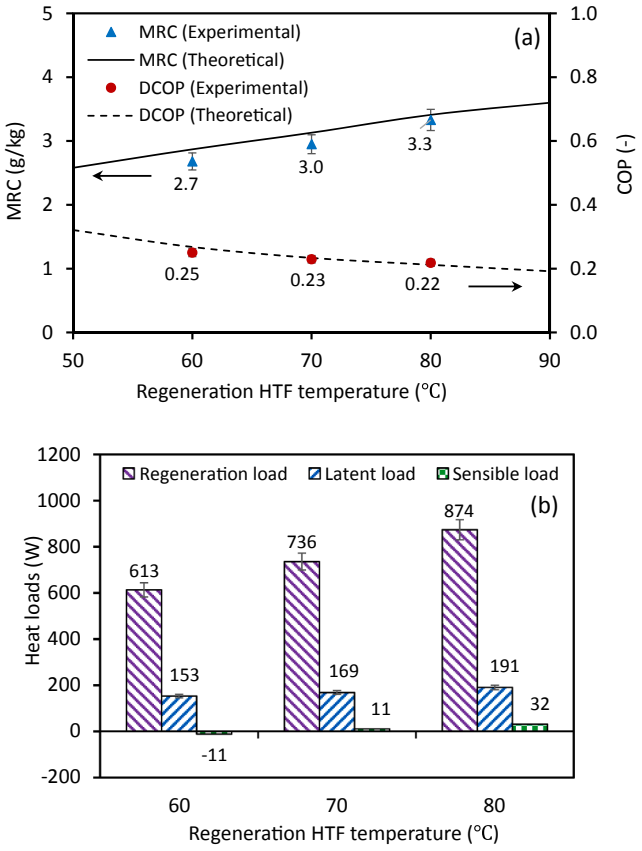

Fig. 10. Effect of regeneration HTF temperature on the (a) MRC and COP obtained by theoretical and experimental analyses and (b) heat loads of DC-HX including required regeneration heat, latent heat removal from the greenhouse and sensible heat added to the greenhouse.

2.6 to 3.0 g/kg, i.e., about 15% improvement. This trend is attributed to the slight improvement in the effective removal of adsorption heat by the cooling HTF. When the cooling HTF temperature increases, the heat of adsorption is not effectively removed, and there is a decrease in adsorption capacity of the desiccant.

- COP also increases from 0.20 to 0.23 due to higher latent heat removal capacity.
- By applying cooling HTF in the range of 10–25°C, the greenhouse air is heated up, i.e., 11–81 W sensible heating.
- It should be noted that due to HTF temperature is not lower enough than inlet air, the sensible heat is added to the greenhouse space.
- At lower cooling HTF temperatures, a higher temperature gradient exists between the cooling HTF and desiccant, thereby reducing the sensible heating load.
- Regeneration and latent heat loads decrease with the increase of cooling HTF temperature. This is due to the fact that a considerable portion of the regeneration load is dedicated to heating up the heat exchanger due to thermal inertia and also residual cooling HTF during the regeneration process.

4.6. *Effect of regeneration HTF temperature*

The effect of regeneration HTF temperature on the MRC, COP, latent heat, sensible heat, and regeneration heat of the present DC-HX is shown in Fig. 10. The following can be concluded:

- The temperature of hot HTF has an important influence on the regeneration process of DC-HX and makes a further effect on the humidity and temperature of supply air.
- Elevated regeneration HTF temperature has a beneficial impact on MRC and negative impact on COP. As regeneration HTF temperature rises from 60 to 80°C, the MRC increases from 2.7 to 3.3 g/kg, i.e., 22% improvement, while COP declines from 0.25 to 0.22.
- As analyzed above, higher heating HTF temperature leads to larger dehumidification capacity, which means that DC-HX can process more latent load.
- The moisture transfer potential between the air stream and desiccant increases significantly at higher regeneration temperatures. As a result, the desiccant is more completely regenerated and can adsorb more moisture in one adsorption cycle.
- Latent load increases as the regeneration HTF temperature increments under given conditions. The surface of solid desiccant becomes drier at the end of the regeneration process with the rising of regeneration temperature, which increases the moisture removal.
- Temperature of outlet air keeps increasing with increasing temperature of hot HTF, because more thermal energy is transferred to air side, thereby elevating sensible heat.
- Regeneration load increases as the regeneration HTF temperature increments due to required more heating power.
- The increase of regeneration HTF temperature has more effect on the rise of sensible load than latent load, which reflects on the tendencies of temperature and humidity ratio of supply air, respectively.

4.7. *Optimization and comparison*

In this paper, MRC and COP are considered as objective functions. These objectives are considered simultaneously in a multi-objective optimization process. The goal is to maximize the MRC and COP in

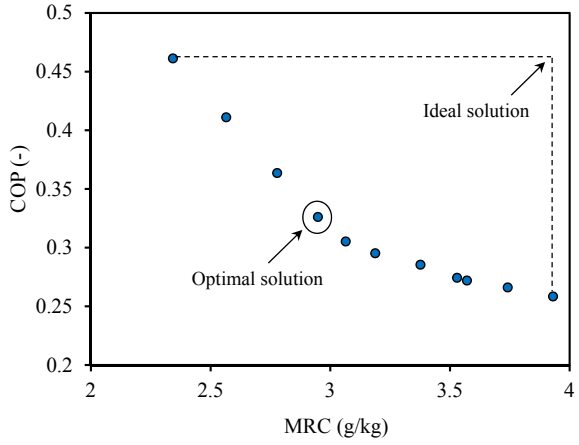

Fig. 11. Pareto front curve for two objective functions (MRC and COP).

terms of the five operating parameters, i.e., air flow rate, temperature, RH, as well as the HTF temperatures using genetic algorithm technique.

Eq. (1) shows how a multi-objective optimization problem can be formulated mathematically.

$$\begin{cases} Find\ x = (\mathrm{x_i}),\ \forall i = 1, 2, \cdots, \mathrm{N_{par}} \\ Minimize/Maximize\ \mathrm{f_i(x)},\ \forall i = 1, 2, \cdots, \mathrm{N_{obj}} \\ \mathrm{g_j(x)} = 0,\ \forall j = 1, 2, \cdots, j \\ \mathrm{h_k(x)} \le 0,\ \forall k = 1, 2, \cdots, k \end{cases} \tag{11}$$

where x represents a vector containing N_{obj} the number of objectives, $f_i(x)$ the objective functions, the N_{par} design parameters and also, $g_j(x)$ and $h_k(x)$ are equality and inequality constraints. In this paper, genetic algorithm technique for optimizing the objective functions has been implemented.

It should be noted that a decision-making method is required to choose a point on Pareto front curve as an optimal point. Various procedures are proposed to pick the optimal solution from the Pareto frontier. Regarding to the possibility of different objectives' dimensions, scales and dimensions of objectives space have to be unified. On the other hand, before the decision making procedure, objectives vectors have to be non-dimensional. Euclidian non-dimensional technique has been used in this research [31,32]. In this method, a non-dimensionalized objective, F_{ij}^{n} is defined as,

$$F_{ij}^{n} = \frac{F_{ij}}{\sqrt{\sum_{i=1}^{m} \left(F_{ij}\right)^2}} \tag{12}$$

The optimal operating parameters are a set of diversified optimum points, called 'Pareto optimal fronts', which are shown in Fig. 11. Indeed, all points on the figure could potentially be an optimum result, and choosing the ultimate optimum point is dependent on the significance of each objective for decision-makers. In this study, the linear programming technique for a multidimensional analysis of preference (LINMAP) was employed to choose the final point from the Pareto optimal front [33]. In the LINMAP method, after Euclidian non-dimensionalization of all objectives, the spacial distance of each solution on the Pareto frontier from the ideal point denoted by $\mathrm{d_{i+}}$ is determined as follow,

$$d_{i+} = \sqrt{\sum_{j=1}^{n} \left(F_{ij} - F_{j}^{ideal}\right)^2} \tag{13}$$

where n denotes the number of objective while i stand for each solution on the Pareto frontier (i = 1, 2, …, m). In Eq. (13), F_j^{ideal} is the ideal value for j^{th} objective obtained in a single-objective optimization. In LINMAP method, the point with the lowest distance from the ideal point on the Pareto frontier is chosen as the ultimate optimal solution. In fact,

Table 5
Comparison of MRC and COP of DC-HXs in our study with those in the literature.

Literature	Desiccant material	Constant parameters	Changing parameter	MRC (g/kg)	COP
Our study	FAM-Z02	$T_a = 20^\circ$C $T_c = 10^\circ$C $T_h = 70^\circ$C $RH = 60\%$ $V_a = 40$ *CFM*	$V_a = 20 \rightarrow 80$ CFM	3.4 → 2.3	0.21 → 0.22
			RH = 40 → 90%	2.1 → 4.7	0.16 → 0.35
			$T_a = 10 \rightarrow 30^\circ$C	1.6 → 5.4	0.15 → 0.52
			$T_h = 50 \rightarrow 90^\circ$C	2.9 → 3.6	0.32 → 0.19
			$T_c = 5 \rightarrow 30^\circ$C	3.1 → 2.3	0.25 → 0.19
Ge et al. [24]	Silica gel Polymer	$T_a = 30^\circ$C $T_c = 25^\circ$C $T_h = 60^\circ$C $Y_a = 14.3$ g/kg	$v_a = 0.5 \rightarrow 2.0$ m/s	3.6 → 1.4 1.6 → 0.7	0.31 → 0.48 0.22 → 0.30
			$Y_a = 10 \rightarrow 17.5$ g/kg	1.0 → 3.8 0.4 → 2.0	0.28 → 0.55 0.23 → 0.39
			$T_a = 25 \rightarrow 35^\circ$C	3.2 → 2.9 1.6 → 1.1	0.40 → 0.45 0.31 → 0.35
			$T_h = 60 \rightarrow 80^\circ$C	3.1 → 5.0 1.4 → 2.9	0.43 → 0.48 0.33 → 0.22
Zhao et al. [34]	Silica gel	$T_a = 29 - 31^\circ$C $T_c = 24 - 28^\circ$C $T_h = 80 - 85^\circ$C $Y_a = 17 - 18$ g/kg	$T_a = 18 \rightarrow 31^\circ$C	1.2 → 5.9	0.11 → 0.43
			$Y_a = 12 \rightarrow 18$ g/kg	2.7 → 5.5	0.26 → 0.36
Vivekh et al. [35]	Silica gel PVA-LiCl	$T_a = 30^\circ$C $T_c = 30^\circ$C $T_h = 80^\circ$C $Y_a = 21.5$ g/kg $\dot{m}_a = 55$ kg/h	$\dot{m}_a = 35 \rightarrow 65$ kg/h	5.8 → 3.0 7.8 → 4.7	0.21 → 0.11 0.28 → 0.16
			$Y_a = 17.5 \rightarrow 21.5$ g/kg	2.2 → 4.4 3.8 → 5.2	0.06 → 0.14 0.12 → 0.20
			$T_a = 30 \rightarrow 36^\circ$C	4.7 → 4.3 5.2 → 4.5	0.17 → 0.21 0.19 → 0.25
			$T_h = 40 \rightarrow 80^\circ$C	3.0 → 4.7 4.2 → 5.2	0.42 → 0.14 0.58 → 0.20

(*continued on next page*)

Table 5 (*continued*)

Literature	Desiccant material	Constant parameters	Changing parameter	MRC (g/kg)	COP
			$T_c = 25 \rightarrow 35°C$	4.8 → 3.7	0.18 → 0.09
				6.7 → 4.0	0.25 → 0.18

optimization of each objective is regardless to the other objectives' satisfaction. In this regard, the optimal point obtained by this method has been taken as the final optimal design point in this research. The MRC and COP of the present DC-HX at the selected optimum point is 2.9 g/kg and 0.33, respectively. The magnitudes of optimal airflow rate, temperature, RH, cold HTF temperature, and regeneration HTF temperature are 40 CFM, 25°C, 80%, 10°C, and 65°C, respectively.

In order to highlight the competitiveness of our DC-HX coated with AQSOA™-FAM-Z02, its performance was compared with that in the literature. Table 5 shows the MRC and thermal COP of the DC-HXs in our study along with some of the studies in the literature. It can be concluded that DC-HX coated with AQSOA™-FAM-Z02 performs well in terms of dehumidification capability as well as thermal performance compared to other DC-HXs.

5. Conclusions

The feasibility of using a new AQSOA™-FAM-Z02 DC-HX for greenhouse dehumidification has been studied. A theoretical modeling, experimental analysis, and a parametric study have been performed to investigate the effects of operating variables such as greenhouse air flow rate, temperature, and RH, as well as regeneration and cooling HTF temperatures on the MRC and COP of the proposed DC-HX. Moreover, the share of latent heat and sensible heat handled by the present DC-HX has been evaluated. Finally, optimal operating parameters to maximize COP and MRC have been determined using a genetic algorithm. The main findings can be summarized as:

- In order to achieve optimum performance, an effective cycle time is defined and used. Thus, optimal adsorption and regeneration time for the baseline condition are 40 and 20 min, respectively.
- Decreasing the greenhouse airflow rate leads to an enhanced MRC, but its effect on the COP is negligible.
- MRC and COP improves with an increment of greenhouse air temperature and RH and decrease of cooling HTF temperature.
- Elevated regeneration HTF temperature has a beneficial impact on the MRC and negative impact on COP. As regeneration temperature rises from 60 to 80°C, the MRC increases from 2.7 to 3.3 g/kg, i.e., a 22% improvement, while COP declines from 0.25 to 0.22.
- DC-HX can achieve MRC and COP in the range of 2.5–4.0 and 0.18–0.3, thereby providing competitive performance in greenhouse conditions.
- Latent load (dehumidification) and sensible load (cooling/heating) can be independently handled by the desiccant film and the heat transfer medium, respectively. In other words, the outlet air of DC-HX can directly satisfy the supply air requirements.
- Optimal operating parameters to maximize COP and MRC for the present DC-HX are determined by a multi-objective optimization using genetic algorithm. The corresponding MRC and COP at the selected optimum point are 2.9 g/kg and 0.33, respectively.

Declaration of Competing Interest

The authors declare that they have no known competing financial interests or personal relationships that could have appeared to influence the work reported in this paper.

Acknowledgment

The authors gratefully acknowledge the financial support from the Natural Sciences and Engineering Research Council of Canada, College-University Idea to Innovation Grant "From Waste to Clean Food" (NSERC CUI2I 501951-16) and the Canadian Queen Elizabeth II Diamond Jubilee Scholarships (QES). The QES is managed through a unique partnership of Universities Canada, the Rideau Hall Foundation (RHF), Community Foundations of Canada (CFC), and Canadian universities. The QES Advanced Scholars (AS) Program is made possible with financial support from the International Research and Development Centre (IDRC) and The Social Sciences and Humanities Research Council of Canada (SSHRC).

References

[1] B. Grace, R. Zentner, Energy Consumption in the Canadian Agricultural and Food Sector, 1998.
[2] https://www.statcan.gc.ca/.
[3] B. Wong, L. McClung, A. Snijders, D. McClenahan, J. Thornton, The application of aquifer thermal energy storage in the Canadian greenhouse industry, Acta Hortic. (2011) 437–444.
[4] B. Mohammadi, F. Ranjbar, Y. Ajabshirchi, Exergoeconomic analysis and multi-objective optimization of a semi-solar greenhouse with experimental validation, Appl. Therm. Eng. 164 (2020), 114563, https://doi.org/10.1016/j.applthermaleng.2019.114563.
[5] E. Romantchik, E. Ríos, E. Sánchez, I. López, J.R. Sánchez, Determination of energy to be supplied by photovoltaic systems for fan-pad systems in cooling process of greenhouses, Appl. Therm. Eng. 114 (2017) 1161–1168, https://doi.org/10.1016/j.applthermaleng.2016.10.011.
[6] A. Vadiee, V. Martin, Energy management in horticultural applications through the closed greenhouse concept, state of the art, Renew. Sustain. Energy Rev. 16 (2012) 5087–5100, https://doi.org/10.1016/j.rser.2012.04.022.
[7] M. Amani, S. Foroushani, M. Sultan, M. Bahrami, Comprehensive review on dehumidification strategies for agricultural greenhouse applications, Appl. Therm. Eng. 181 (2020) 115979, https://doi.org/10.1016/j.applthermaleng.2020.115979.
[8] K. Maslak, S. Nimmermark, Thermal energy use for dehumidification of a tomato greenhouse by natural ventilation and a system with an air-to-air heat exchanger, Agric. Food Sci. 26 (2017) 56, https://doi.org/10.23986/afsci.58936.
[9] J. Campen, G.P. Bot, Determination of greenhouse-specific aspects of ventilation using three-dimensional computational fluid dynamics, Biosyst. Eng. 84 (2003) 69–77, https://doi.org/10.1016/S1537-5110(02)00221-0.
[10] M. Sultan, T. Miyazaki, B.B. Saha, S. Koyama, Steady-state investigation of water vapor adsorption for thermally driven adsorption based greenhouse air-conditioning system, Renew. Energy. 86 (2016) 785–795, https://doi.org/10.1016/j.renene.2015.09.015.
[11] K. Ghali, Energy savings potential of a hybrid desiccant dehumidification air conditioning system in Beirut, Energy Convers. Manag. 49 (2008) 3387–3390, https://doi.org/10.1016/j.enconman.2008.04.014.
[12] P. Vivekh, M. Kumja, D.T. Bui, K.J. Chua, Recent developments in solid desiccant coated heat exchangers – A review, Appl. Energy. 229 (2018) 778–803, https://doi.org/10.1016/j.apenergy.2018.08.041.
[13] A. Saeed, A. Al-Alili, A review on desiccant coated heat exchangers, Sci. Technol. Built Environ. 23 (2017) 136–150, https://doi.org/10.1080/23744731.2016.1226076.
[14] S.J. Oh, K.C. Ng, W. Chun, K.J.E. Chua, K. Choon Ng, K. Thu, M. Kum Ja, M. R. Islam, W. Chun, K.J.E. Chua, Evaluation of a dehumidifier with adsorbent coated heat exchangers for tropical climate operations, Energy 137 (2017) 441–448, https://doi.org/10.1016/j.energy.2017.02.169.
[15] Z. Li, S. Michiyuki, F. Takeshi, Experimental study on heat and mass transfer characteristics for a desiccant-coated fin-tube heat exchanger, Int. J. Heat Mass Transf. 89 (2015) 641–651, https://doi.org/10.1016/j.ijheatmasstransfer.2015.05.095.
[16] Y. Zhao, Y.J. Dai, T.S. Ge, H.H. Wang, R.Z. Wang, A high performance desiccant dehumidification unit using solid desiccant coated heat exchanger with heat recovery, Energy Build. 116 (2016) 583–592, https://doi.org/10.1016/j.enbuild.2016.01.021.
[17] T.S. Ge, J.Y. Zhang, Y.J. Dai, R.Z. Wang, Experimental study on performance of silica gel and potassium formate composite desiccant coated heat exchanger, Energy 141 (2017) 149–158, https://doi.org/10.1016/j.energy.2017.09.090.
[18] A.S. Valarezo, X.Y. Sun, T.S. Ge, Y.J. Dai, R.Z. Wang, Experimental investigation on performance of a novel composite desiccant coated heat exchanger in summer and winter seasons, Energy 166 (2019) 506–518, https://doi.org/10.1016/j.energy.2018.10.092.
[19] L.M. Hu, T.S. Ge, Y. Jiang, R.Z. Wang, Performance study on composite desiccant material coated fin-tube heat exchangers, Int. J. Heat Mass Transf. 90 (2015) 109–120, https://doi.org/10.1016/j.ijheatmasstransfer.2015.06.033.

[20] T.S. Ge, Y.J. Dai, R.Z. Wang, Performance study of silica gel coated fin-tube heat exchanger cooling system based on a developed mathematical model, Energy Convers. Manag. 52 (2011) 2329–2338, https://doi.org/10.1016/j.enconman.2010.12.047.
[21] T.S. Ge, Y.J. Dai, R.Z. Wang, Performance study of desiccant coated heat exchanger air conditioning system in winter, Energy Convers. Manag. 123 (2016) 559–568, https://doi.org/10.1016/j.enconman.2016.06.075.
[22] S. Chai, X. Sun, Y. Zhao, Y. Dai, Experimental investigation on a fresh air dehumidification system using heat pump with desiccant coated heat exchanger, Energy. 171 (2019) 306–314, https://doi.org/10.1016/j.energy.2019.01.023.
[23] M.J. Goldsworthy, Measurements of water vapour sorption isotherms for RD silica gel, AQSOA-Z01, AQSOA-Z02, AQSOA-Z05 and CECA zeolite 3A, Microporous Mesoporous Mater. 196 (2014) 59–67, https://doi.org/10.1016/j.micromeso.2014.04.046.
[24] T.S. Ge, Y.J. Dai, R.Z. Wang, Z.Z. Peng, Experimental comparison and analysis on silica gel and polymer coated fin-tube heat exchangers, Energy. 35 (2010) 2893–2900, https://doi.org/10.1016/j.energy.2010.03.020.
[25] S.J. Slayzak, J.P. Ryan, Desiccant Dehumidification Wheel Test Guide, Golden, CO (United States) (2001), https://doi.org/10.2172/775748.
[26] A. Freni, B. Dawoud, L. Bonaccorsi, S. Chmielewski, A. Frazzica, L. Calabrese, G. Restuccia, Characterization of Zeolite-Based Coatings for Adsorption Heat Pumps, Springer International Publishing, Cham, 2015. https://doi.org/10.1007/978-3-319-09327-7.
[27] B. Dawoud, On the effect of grain size on the kinetics of water vapor adsorption and desorption into/from loose pellets of FAM-Z02 under a typical operating condition of adsorption heat pumps, J. Chem. Eng. Japan 40 (2007) 1298–1306, https://doi.org/10.1252/jcej.07WE163.
[28] S.K. Henninger, F.P. Schmidt, H.-M. Henning, Water adsorption characteristics of novel materials for heat transformation applications, Appl. Therm. Eng. 30 (2010) 1692–1702, https://doi.org/10.1016/j.applthermaleng.2010.03.028.
[29] C. Elliott, V. Vijayakumar, W. Zink, R. Hansen, National instruments LabVIEW: a programming environment for laboratory automation and measurement, J. Assoc. Lab. Autom. 12 (2007) 17–24, https://doi.org/10.1016/j.jala.2006.07.012.
[30] S. Kline, F. McClintock, Describing uncertainties in single sample experiments, Mech. Eng. 78 (1953) 3–8.
[31] V. Srinivasan, A.D. Shocker, Linear programming techniques for multidimensional analysis of preferences, Psychometrika 38 (1973) 337–369.
[32] Z. Yue, A method for group decision-making based on determining weights of decision makers using TOPSIS, Appl. Math. Model. 35 (2011) 1926–1936, https://doi.org/10.1016/j.apm.2010.11.001.
[33] U. Dave, D.L. Olson, Decision aids for selection problems, J. Oper. Res. Soc. 48 (1997) 541, https://doi.org/10.2307/3010514.
[34] Y. Zhao, T.S. Ge, Y.J. Dai, R.Z. Wang, Experimental investigation on a desiccant dehumidification unit using fin-tube heat exchanger with silica gel coating, Appl. Therm. Eng. 63 (2014) 52–58, https://doi.org/10.1016/j.applthermaleng.2013.10.018.
[35] P. Vivekh, D.T. Bui, Y. Wong, M. Kumja, K.J. Chua, Performance evaluation of PVA-LiCl coated heat exchangers for next-generation of energy-efficient dehumidification, Appl. Energy 237 (2019) 733–750, https://doi.org/10.1016/j.apenergy.2019.01.018.